

Repetitive extreme-acceleration (14-g) spatial jumping with Salto-1P

Duncan W. Haldane*, Justin K. Yim*, and Ronald S. Fearing

Abstract—In this work we present a new robotic system, Salto-1P, for exploring extreme jumping locomotion. Salto-1P weighs 0.098 kg, and has an active leg length of 14.4 cm. The robot is able to perform a standing vertical leap of 1.25 m, continuously hop to heights over 1 m, and jump over 2 m horizontally. Salto-1P uses aerodynamic thrusters and an inertial tail to control its attitude in the air. A linearized Raibert step controller was sufficient to enable unconstrained in-place hopping and forwards-backwards locomotion with external position feedback. We present studies of extreme jumping locomotion in which the robot spends just 7.7% of its time on the ground, experiencing accelerations of 14 times earth gravity in its stance phase. An experimentally collected dataset of 772 observed jumps was used to establish the range of achievable horizontal and vertical impulses for Salto-1P.

I. INTRODUCTION

Saltatorial animals (animals that locomote by jumping) such as bushbabies can move through complex, usually arboreal environments by chaining together large (over 2 meter) jumps. This saltatorial mode of locomotion is interesting for robotics because it enables rapid movement through complex terrain and added flexibility for how the robot interacts with the environment. The farther a robot can jump the better it can discretize its environment, clearing larger gaps and obstacles and making path-planning easier [7]. Prior work has shown that a robot that can perform two high-amplitude jumps in succession was able to spring off a wall to gain energy and height [12]. A robot proficient at saltatorial locomotion would be able to move through its environment in new and previously insupposable ways.

Extreme saltatorial locomotion is characterized by large jumps (over 1m) and short stance times which presents some challenges. To explore this mode of locomotion a robot needs to be able to jump high, do it repeatedly, and control its landings. Should those criteria be met, extreme saltatorial locomotion may still present unknown challenges and properties.

For instance: duty factor is defined as the ratio of time spent on the ground to the total stride duration, and is frequently used to assess the dynamic character of a gait.

This material is based upon work supported by the National Science Foundation under IGERT Grant No. DGE-0903711, the NSF GRFP, NSF CMMI 1549667, and the United States Army Research Laboratory under the Micro Autonomous Science and Technology Collaborative Technology Alliance.

D.W. Haldane is with the Department of Mechanical Engineering, University of California, Berkeley, CA 94720 USA dhaldane@berkeley.edu

J.K. Yim, and R.S. Fearing are with the Department of Electrical Engineering and Computer Sciences, University of California, Berkeley, CA 94720 USA {yim, ronf}@eecs.berkeley.edu

* These authors contributed equally to this work

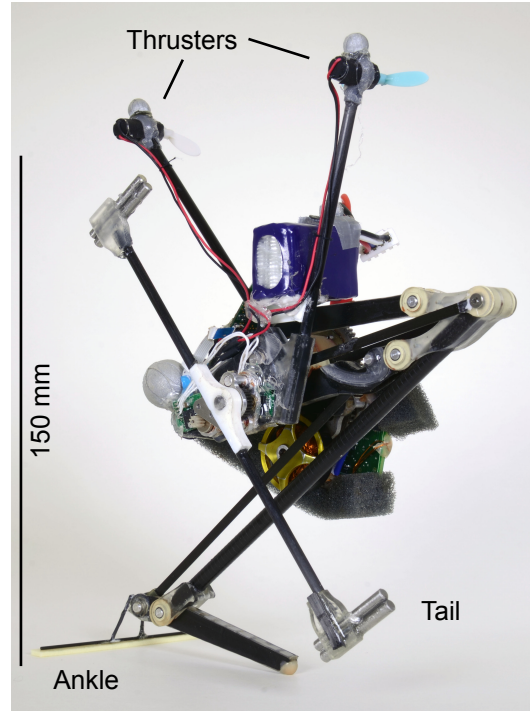


Fig. 1: Photograph of Salto-1P with thrusters, fully crouched. Photo credit: Ethan Schaler.

Typical duty factors for running animals range from 0.36-0.5 [10], and most running robots have a duty factor of approximately 0.5. The robot developed in this work had a duty factor as low as 0.077, lower than the lowest observed duty factor for a *single* limb of a cheetah running at top speed [15]. The accelerations the robot experienced in stance repeatedly exceeded 14 times earth gravity.

There have been many high performance legged robots, but none that are sufficiently specialized for the study of extreme saltatorial locomotion. Power-autonomous running robots capable of repeated jumping [17], [5], [11], [14], [19], [24], [34] have not demonstrated the ability to jump more than 0.5m in height (except Salto-1P (this work)). The jump height of these robots is on-par with their characteristic dimensions, and their relatively small maximal jumps do not enable the agile locomotion proposed by Campana and Laumond [7].

The highest jumping robots explosively release pre-stored energy to power their jumps. This stored energy can be a chemical propellant in robots that use literal explosions to jump, such as the Sandia hopper [31] or the SandFlea from Boston Dynamics. Other high-jumping robots store energy in a parallel-elastic leg mechanism, and use a mechanical

escapement to convert it into kinetic energy in a single burst [20], [6], [35], [28], [1], [22], [29], [23], [33], [18], [32]. At present, all power-autonomous robots (except Salto [12] and Salto-1P) that can jump over 1 meter in height use a parallel-elastic or explosion driven strategy. The issue with these robots is that they cannot perform the controlled, repeated jumps requisite for continuous locomotion. The high-jumping parallel-elastic robots need to wind-up for an extended number of seconds to prepare for their next jump; the behavior has not yet been demonstrated in an explosion-powered robot, perhaps because the jumping appendage is too rigid to allow a stance time long enough to meaningfully interact with the ground.

Previous work has shown that Salto (Expansion: Saltatorial Locomotion on Terrain Obstacles), a robot with a series-elastic actuator and a variable mechanical-advantage (SE+MA) limb (see [13], [12], [25] for design details), can jump over 1 meter in height. The SE+MA actuation strategy allowed the robot to reach this height without a lengthy wind-up period, and without hampering the controllability of the leg with a mechanical escapement or reliance on explosive chemical propellants. The major shortcoming of Salto was that it was purely planar. Any perturbation away from its plane of operation could not be rejected and so the robot could only perform behaviors with small numbers of jump without falling over. Furthermore, Salto only had proprioceptive sensing and lacked a controller that would enable it to perform an extended series of repeated jumps.

In this work, we enable the study of extreme saltatorial locomotion by creating an improved version of Salto, Salto-1P, with full attitude control. We implement the simple Raibert controller [26] to enable Salto-1P to jump repeatedly on a horizontal surface, and explore the range of impulses that can be generated by single stance events.

Section II outlines the development of the robotic hardware, attitude controllers, locomotion controller and experimental procedure. Results for attitude control and jumping experiments are given in Section III, and conclusions are discussed in Section IV.

II. METHODS

A. Attitude control

The first challenge for Salto-1P was to enable attitude control, so that the spatial touchdown angle of the leg could be modulated. The original Salto was planar, and used a mass-balanced inertial tail to control its orientation in the sagittal plane [12]. This tail powered the aggressive attitude repositioning required to perform the wall-jump maneuver [12]. For Salto-1P we decided to retain the balanced tail for rapid sagittal reorientation and minimally supplement it with enough control authority to keep the robot upright, with the correct yaw heading. A challenge for stabilizing extreme-acceleration jumping is the short stance duration relative to flight time. Any stabilization method operating only in stance (like a foot or articulated ankle) must correct the attitude during the 0.05s stance and reduce the take-off angular velocity error low enough that the robot is within a

few degrees of its desired touchdown angle at the next stance event, 0.5s later.

There have been numerous stabilization methods for monopoedal robots (see Sayyad et al. for a review [27]). For testing purposes, most commonly a monopode is mounted to a boom, which is unsuitable for Salto-1P due to the low mass of the robot and the magnitude of its vertical excursions. Another option is to mount the leg on a two degree-of-freedom servo joint at the center of mass of the body of the robot, as was done for the Raibert Hopper [26] and the 3D Bow Leg Hopper [34]. This is unattractive for Salto-1P because the movement range of the body becomes limited, greatly limiting the angular impulses it can reject. Any reorientation strategy with an offset mass (such as a 2 DoF tail [8]) presents difficulties for Salto-1P due to characteristically large accelerations in stance that create large torque requirements on the tail actuators. Other monopodes (e.g. [16][30]) opt for statically stable feet and avoid jumps that would cause the robot to leave its support polygon. This approach is untenable for Salto-1P, which can jump two meters horizontally.

Several jumping robots use aerodynamic surfaces to glide after jumping [32][21][9]. Aerodynamic surfaces are attractive for their low mass and ability to apply force while airborne (not just in stance). A drawback is the large requisite size at the Reynolds numbers associated with terrestrial locomotion, and that force they apply is velocity-dependent so a robot jumping vertically loses control authority at apex. We opted for a compact aerodynamic-stabilization method that does not rely on body velocity by using the thrusters seen in Fig. 1. These thrusters are commercial mini-quadcopter (*Cheerson CX-10*) propeller blades mounted in a ‘V’ configuration, with moment arms about the center of mass that prioritize control over roll angle (80mm) over yaw angle (40mm). Roll torque is created by driving both thrusters in the same direction; yaw torque is generated with a differential motor command. The thruster assembly successfully stabilized the robot (see Figs. 4 and 5), and had a net mass of 0.0044 kg.

B. Robotic Hardware

Salto-1P is an improved version of the Salto robot [12]. The series elastic actuator and mechanism geometry from Salto have been preserved in Salto-1P. However, some of the links have been reshaped to allow Salto-1P to get lower in crouch than Salto, to increase the achievable jump height by enhancing the power-modulating effect of the linkage [13]. The body was also redesigned using topology optimization to create a highly mass-efficient, low compliance structure. The tail gearbox has been upgraded to steel gears with an aluminum housing in Salto-1P, after observing that Salto’s plastic tail gearbox was a source of much unreliability [12].

Like Salto, Salto-1P is controlled with the ImageProc 2.5¹ robot control board [2]. The tail and thruster motors are driven from onboard H-bridges. Salto-1P uses a customized

¹Embedded PCB: https://github.com/biomimetics/imageproc_pcba

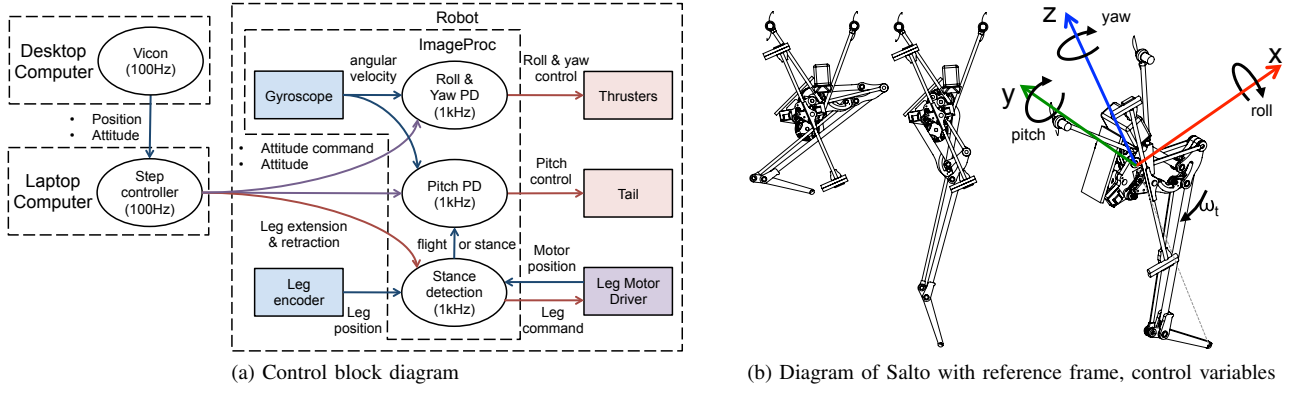


Fig. 2: Overall system block diagram and reference frame of Salto-1P

BLDC motor driver, which is smaller and lower mass than the COTS driver used by Salto. The imageProc records telemetry from the motor driver, and an onboard 6-axis IMU at 1 kHz.

Salto-1P contacts the ground with a hemispherical rubber toe (IE7000, *Innovative polymers*). A sample of the toe material was rubbed on a sample of the carpet from the test chamber while a force-sensor (nano43, *ATI*) recorded data to determine the frictional coefficient, $\mu = 0.79$. This coefficient of friction was sufficiently high that the toe did not slip during experiments. When the robot is fully crouched, it rests on an ankle structure, seen in Fig. 1, that allows a statically-stable rest position. The height of this ankle is such that the center of mass is located behind the toe of the robot.

C. Jumping controller

Salto was designed as a literal instantiation of the spring-loaded inverted pendulum (SLIP) model of running [4], so that the control of the platform could be made as simple as possible. The goal was to have Salto appear dynamically as a point mass on a spring-loaded massless leg. Salto's toe point moves in a straight line, the mass of the leg was minimized, the leg mechanism was balanced so that motion of the links produces no body rotation, the inertial tail is mass balanced, and the mass of the body was centralized [13], [25]. This is an opposite design approach to the Acrobot jumper that used a minimal mechanical design with non-linear control, and could barely slide while maintaining balance [3]. Designed in this way, Salto resembles an untethered, 0.098 kg version of the Raibert hopper [26] that has one of the leg angle

positioning servos replaced with thrusters, has control over its yaw heading, and can jump 1.25m high.

Seeking the simplest solution, we elected to implement a linearized controller based on the Raibert step controller [26] for our initial experiments.

As in the Raibert step controller, control is decoupled into three parts: hopping height, tail velocity, and horizontal velocity.

Hopping height is set by applying a fixed thrust on the ground. Raibert showed in [26] that this fixed thrust strategy converges to a unique steady state apex height for each thrust value. Thrust is specified by selecting the leg retraction length before touchdown and a leg extension distance that is triggered when the robot contacts the ground (detected by monitoring the deflection of the spring in the series-elastic actuator).

Salto-1P's balanced tail is analogous to the balanced body of Raibert's hopping machine. However, since the tail rotates without limit, its angle is unimportant and we are concerned only with its angular velocity. During stance phase, the H-bridge driving the tail motor is put in brake mode to slow down the tail. This is important for maintaining control authority: the control torque the tail can produce decreases linearly with tail speed. Without braking, the tail accelerates to the free-running speed of the motor, and the robot is unable to maintain control of its locomotion.

Horizontal velocity is controlled by selection of an appropriate leg angle at touchdown. For simplicity, we use yaw-roll-pitch Euler angles to parameterize rotation. The robot-attached reference frame is shown in Fig. 2b. Since Salto-1P's inertial tail grants greater control authority about the pitch axis than the thrusters provide about the roll axis, maneuvers are guided to the sagittal plane and the desired yaw angle is 0. Given the desired CG positions and velocities, the touchdown roll and pitch angles are selected by:

$$\begin{aligned}\phi &= -k_{Px} \text{sat}(x_d - x, x_{max}) - k_{Vx}(\dot{x}_d - \dot{x}) \\ \theta &= k_{Py} \text{sat}(y_d - y, y_{max}) + k_{Vy}(\dot{y}_d - \dot{y})\end{aligned}$$

Where ϕ is the pitch angle, θ is the roll angle, and $\text{sat}(u)$ is the saturation function that limits the angle command due to position error. x is the position coordinate in the sagittal plane, y is the lateral coordinate.

TABLE I: ROBOTIC PLATFORM METRICS

	Salto[12]	Salto-1P
Mass (kg)	0.1000	0.0981
Active leg Length (m)	0.138	0.144
Maximum jump height (m)	1.007	1.252
Vertical jumping agility (m/s)	1.75	1.83
<i>Max control torque (Nm):</i>		
Pitch	0.029	0.034
Roll	0	0.0078
Yaw	0	0.0039

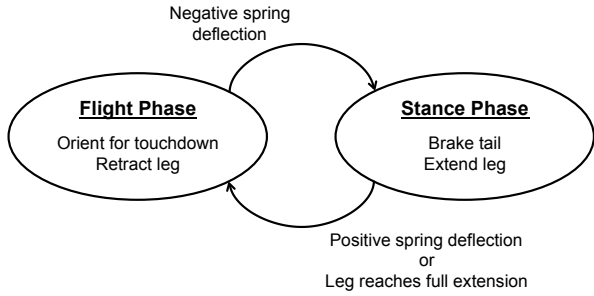


Fig. 3: Stance and Flight control.

D. Experimental procedure

To test the stabilizing capacity of attitude controlling actuators, the robot was suspended from the yaw, pitch, and roll axes in turn and was given impulse disturbances by hand. During this experiment the attitude controller tried to maintain a fixed angle; the angular perturbation and subsequent recovery was observed with external motion tracking (*Optitrack*). The size of the impulse was estimated using data from the on-board gyroscope.

Jumping experiments were conducted in a Vicon motion capture environment in order to provide position feedback. The trackable area in the room measures 2 by 3 meters on the ground. Vicon position and orientation measurements were passed at 100Hz to the ground station running in ROS on a laptop computer. The ground station estimated body velocity from the Vicon position measurement by discrete differentiation with a low pass filter. The ground station calculated the desired leg lengths and touchdown angles using the step controller detailed above and sent these commands along with the Vicon attitude measurement to the robot over an XBee radio connection. Sending the Vicon measured attitude, as well as an attitude command, prevents the onboard attitude estimate from drifting due to gyro integration error. The control flow is shown in Fig. 2a.

III. RESULTS

A. Attitude stabilization

Fig. 4 shows 5% recovery time vs. perturbation impulse for Salto-1P in yaw, pitch, and roll. Salto-1P recovers from perturbations in pitch more quickly than roll or yaw since the inertial tail provides larger torques than the thrusters. Note that the maximum angular impulse the 0.010 kg, 0.14 m inertial tail can reject is limited. It can be no more than $H_t = I\omega$, where I is the inertia of the tail, and ω is the maximum tail angular velocity. $H_t = 3.5 \text{ mNm} - \text{s}$ for the inertial tail on Salto-1P. The thrusters are configured to lend more actuation authority to roll than yaw (see Table I), the result of which is seen in Fig. 4. The robot recovers from a disturbance impulse faster in the roll axis than the yaw axis.

Fig. 5 shows the attitude controller performance during a jumping experiment. The roll and yaw axes (Fig. 5(A),(B)) are under-damped with regular deviations of 0.1 radians from the setpoint. More aggressive gains do not yield better performance because the thruster motors are saturated, as shown in Fig. 5(C). More actuator authority would be needed

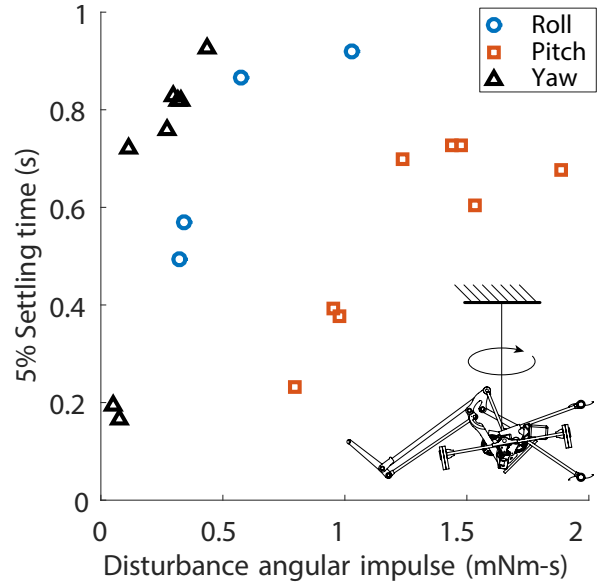


Fig. 4: Time for Salto-1P to stabilize to within 5% of maximum overshoot vs disturbance impulse. Inset cartoon shows experimental setup for roll tests.

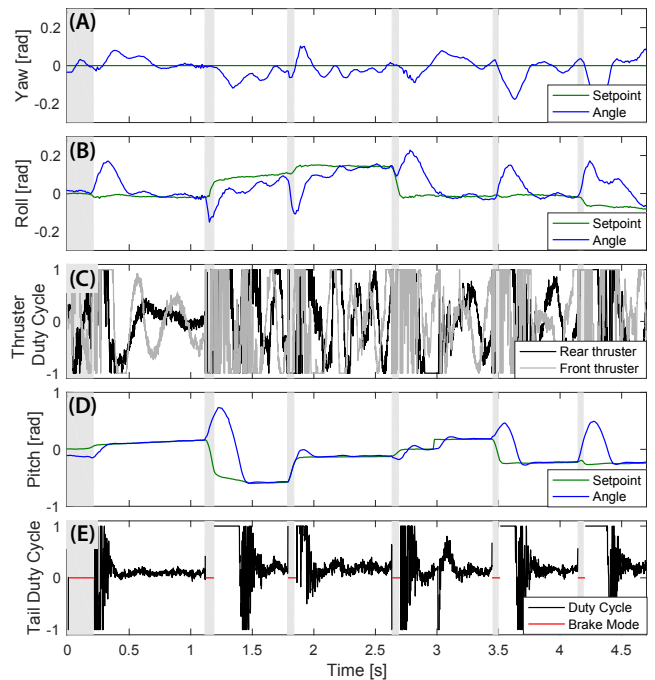
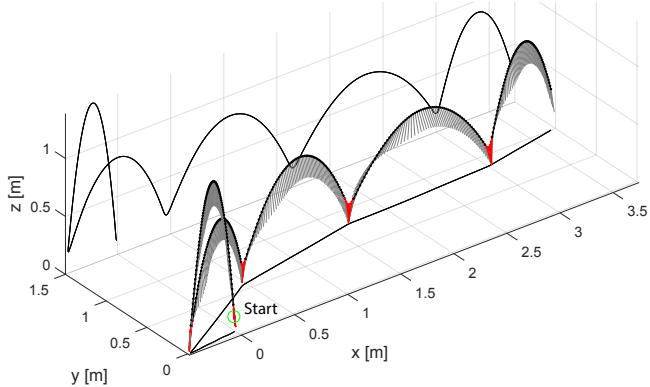


Fig. 5: Attitude controller performance during jumping experiment. (A) Yaw angle and setpoint (B) roll angle and setpoint (C) Thruster motor duty cycle (D) Pitch angle and setpoint (E) Tail motor duty cycle. Stance phases shown in grey.

to improve tracking. The inertial tail affords more control authority, with typical pitch errors at touchdown lower than 0.01 radians, as shown in Fig. 5(D). The tail motor (Fig. 5(E)) brakes during stance phase to slow down. After takeoff, the tail motor applies maximum effort to reposition the body to the next setpoint.



(a) Spatial trajectory of robot center of mass during a jumping experiment. Leg shown as grey in flight, red in stance. Data plotted at 10 ms intervals.



(b) Video stills from high-speed camera footage of first jump of experiment. Time is from onset of activation, aligned with Fig. 7.

Fig. 6: Example data and video stills from forwards-running trial.

B. Saltatorial locomotion

Fig. 6a shows the spatial trajectory of Salto-1P during a forwards jumping experiment. Stills from high-speed video of the same experiment are shown in Fig. 6b. The robot starts fully crouched, statically stable on its ankle, with the center of mass positioned behind the toe. Salto-1P's most energetic jumps occur when it starts in its fully crouched position, where the SE+MA jumping appendage is most fully in effect [13][12]. Because the center of mass is behind the toe, this initial jump is backwards. This starting configuration was used for all of the jumping experiments because the first jump immediately establishes the high energetic state requisite for extreme saltatorial locomotion; the backwards direction perturbs the locomotion controller so that a large range of jumps are explored, and the convergence properties can be studied. The robot exits the trackable range of the experimental test chamber to end this experiment.

Fig. 7(A) shows the height of the center of mass over time for the same trial shown in Fig. 6a, with the stance phases shown in grey. The initial stance phase is the longest at 0.22 s, increased in duration by the SE+MA adaptation [13][12] which allows the robot to jump higher than it would be otherwise able. After the large initial jump, the jump height converges to the lesser height determined by the leg-thrust for this experiment. The average stance duration for this experiment was 0.057 s (not including initial stance); the average flight time was 0.68 s, for an average duty factor of 0.077. The cumulative mechanical work done by the motor

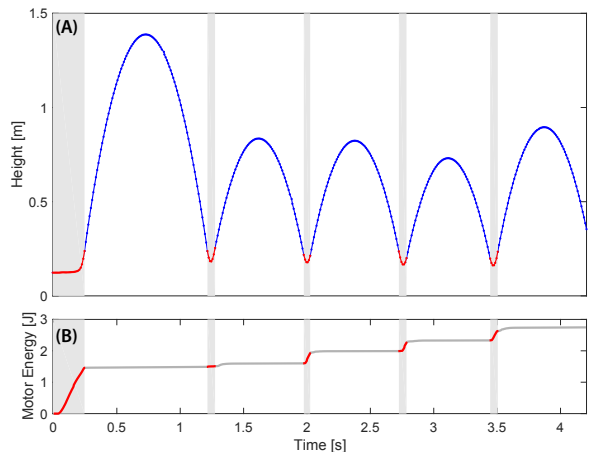


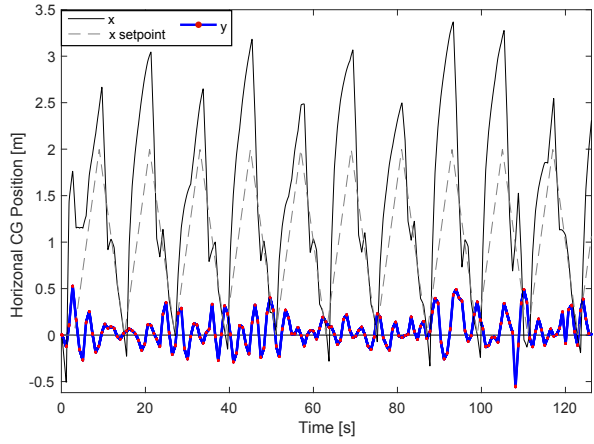
Fig. 7: Energetics of height gain and repeated jumps. Stance periods are shown in grey. (A) height of center-of-mass (B) Cumulative mechanical energy input from motor.

during this experiment is shown in Fig. 7(B). The motor inputs 1.45 J of energy during the initial stance phase, 1.2 J of which appears as extrinsic center of mass energy, for a mechanical efficiency of 83%. The energetic expense of the following jumps is less. The series elastic leg is able to passively store and return an average of 65% of the kinetic energy; the motor inputs 0.3 J per jump to maintain height, overcoming losses from friction and impacts.

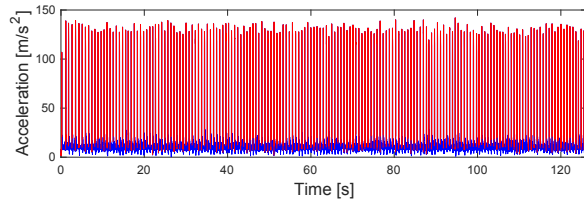
At the fastest observed sustained horizontal speed of 3.6 m/s, the robot's leg motor used 15 J of electrical energy per jump (of which 7 J were used in stance phase) with a jumping period of 0.66 s. 8 J were wasted in flight due to untuned leg controller behavior in the air. This corresponds to a specific resistance of 6.6 for this run.

C. Locomotion controller

The goal of the locomotion controller was to allow Salto-1P to jump repeatedly, to explore the range of accessible jumping behaviors. We performed both in-place jumping tests wherein the robot tries to maintain a fixed $x - y$ position, and forwards-backwards running wherein the desired position is moved forwards and backwards to generate running locomotion. Fig. 8a shows the position of the Salto-1P's center of mass during a forwards-backwards running experiment. Here the controller aims to maintain a 0° yaw heading and zero lateral displacement. The leg thrust in this experiment produces a modest average jump height of 0.65 m. The commanded x position is swept from 0 to 2 m in a sawtooth pattern after an initial 3 second dwell at 0 m. The sawtooth is repeated 10 times during which time Salto-1P makes 174 total jumps. With the exception of several deviations, the lateral position stays within 0.5 m of the desired lateral position. The robot overshoots the sawtooth at the endpoints in the fore-aft direction, where the velocity changes direction. This was caused by aggressive gains on the velocity error of the center of mass that elicited more of the dynamic character of Salto-1P than was appropriate for this locomotion task. The magnitude of Salto-1P's center of mass acceleration is shown in Fig. 8b.



(a) Horizontal position of Salto-1P's center of mass.



(b) Acceleration of Salto-1P's center of mass.

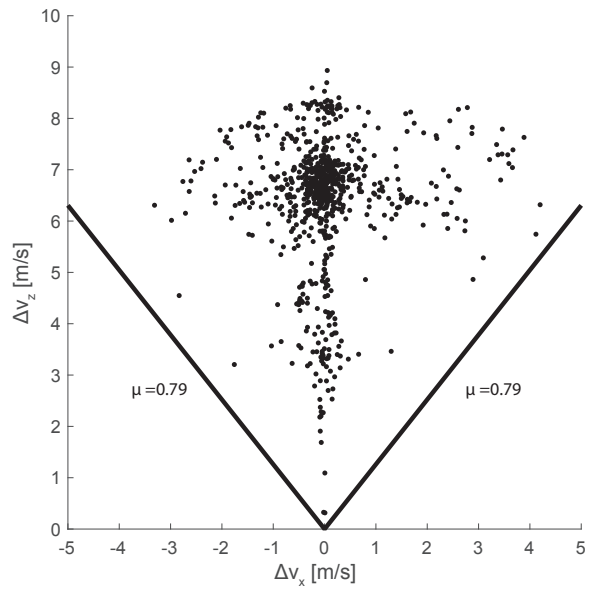
Fig. 8: Motion of robot center of mass during a forwards-backwards jumping experiment (174 total jumps). Red portions of the trace indicate stance periods.

In in-place jumps, Salto-1P maintained foot placements within a region 0.65m laterally and 0.3m sagittally due to the tail's superior pitch authority.

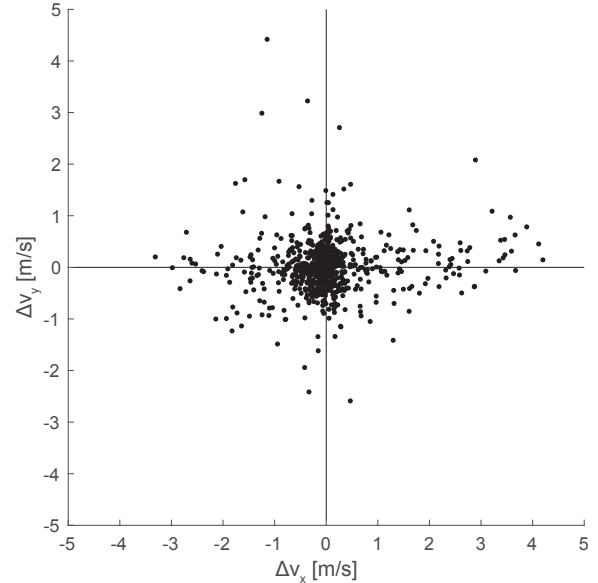
D. Behavior exploration

With the robot operational, we sought to explore the space of feasible jumping behaviors. We ran a series of experiments varying leg thrust commands, and had the locomotion controller issue commands that would perturb the robot from a steady state locomotory behavior. Practically this meant running a forwards-backwards, and in-place hopping experiments with a set of highly-aggressive gains that produced large horizontal velocities.

Fig. 9a shows the vertical and fore-aft impulse for each of the 772 experimentally observed jumps. Most of the data are clustered around $\Delta v_x = 0$, generated from the in-place hopping experiments. Fig. 9b shows lateral vs fore-aft impulses; the data are clustered around $\Delta v_y = 0$ with some spread in Δv_x , driven by the forwards-backwards running experiments. The non-zero horizontal impulses were explored with forwards-backwards running trials, with the largest values found with the most aggressive gains. The largest single impulse was nearly vertical, with a magnitude of $\Delta v = 8.94$ m/s. The robot has trouble jumping below $\Delta v_z = 2$ m/s. The difficulty results because the attitude controlling actuators do not have enough time to reorient the robot before the next stance event. These data are a subset of the attainable jumps; a better exploration scheme would more thoroughly establish the limits of Salto-1P's jumping



(a) Vertical vs fore-aft impulses. Friction cone for measured $\mu = 0.79$ is shown.



(b) Lateral vs fore-aft impulses.

Fig. 9: Impulses for each observed stance period (N=772).

capacity.

IV. CONCLUSION AND FUTURE WORK

In this work we introduced an improved version of a previously developed robot, Salto [12], called Salto-1P. This robot weighs 2 grams less than its predecessor and can jump 0.245 m higher, with a vertical jumping agility of 1.83 m/s, the highest recorded for any battery-powered robot. For this robot we developed a low-mass attitude control scheme that is appropriate for a highly agile, sub 0.1 kg monopedal robot. Two aerodynamic thrusters combined with an inertial tail allowed the robot to control its attitude in the air. The inertial tail was more effective at rejecting perturbations than the thrusters, which were driven to saturation regularly during

the jumping trials. Greater control authority in the roll and yaw axes of the robot would expand the robot's envelope of operation.

The attitude control scheme enabled Salto-1P to execute many (up to 174 in a single trial) jumps in succession on a rigid horizontal surface. A simple linearized controller based on the Raibert step controller was used for global position control of the robot; we demonstrated both in-place hopping and forwards and backwards running. The operation of the attitude actuators in flight phase instead of stance phase meant that much smaller and less powerful actuators could be used; the thrusters could act over several-hundred milliseconds, whereas a ground-based solution would have been limited to the ≈ 50 ms stance duration.

Salto-1P is capable of exploring extreme saltatorial locomotion, demonstrating the ability to continuously jump over 1 meter in height with a duty factor as low as 0.077. Despite the challenges posed by this form of locomotion, selection/construction of appropriate robotic hardware meant that the simple Raibert controller was able to elicit both stable locomotion and a range of dynamic maneuvers. With repeated experiments, we were able to explore the performance envelope for Salto-1P, shown in Fig. 9.

This work has shown that Salto-1P is capable of highly agile locomotion, with a maximum Δv per stance of 8.9 m/s. It has enough raw performance to be an effective platform for experimentally evaluating a recently developed ballistic planning framework [7]. However full control of the platform, particularly landing control to come to a halt and precise foot placement control, is still lacking. Future work will target development of foot placement controllers.

REFERENCES

- [1] R. Armour, K. Paskins, A. Bowyer, J. Vincent, W. Megill, and R. Bomphrey, "Jumping robots: a biomimetic solution to locomotion across rough terrain," *Bioinspir. Biomim.*, vol. 2, no. 3, pp. S65–82, 2007.
- [2] S. S. Baek, F. L. Garcia Bermudez, and R. S. Fearing, "Flight control for target seeking by 13 gram ornithopter," *IEEE Int. Conf. Intell. Robot. Syst.*, pp. 2674–2681, 2011.
- [3] M. D. Berkemeier and R. S. Fearing, "Tracking fast inverted trajectories of the underactuated acrobot," *IEEE Trans. Robot.*, vol. 15, no. 4, pp. 740–750, 1999.
- [4] R. Blickhan, "The spring-mass model for running and hopping," *J. Biomech.*, vol. 22, no. 11-12, pp. 1217–1227, 1989.
- [5] A. Brill, A. De, A. Johnson, and D. Koditschek, "Tail-assisted rigid and compliant legged leaping," *IEEE Int. Conf. Intell. Robot. Syst.*, pp. 6304–6311, 2015.
- [6] J. Burdick and P. Fiorini, "Minimalist jumping robots for celestial exploration," *Int. J. Rob. Res.*, vol. 22, no. 7-8, pp. 653–674, 2003.
- [7] M. Campana and J.-P. Laumond, "Ballistic motion planning," in *IEEE Int. Conf. Intell. Robot. Syst.*, 2016, pp. 1410–1416.
- [8] E. Chang-Siu, T. Libby, M. Brown, R. J. Full, and M. Tomizuka, "A nonlinear feedback controller for aerial self-righting by a tailed robot," in *IEEE Int. Conf. Intell. Robot. Syst.*, 2013, pp. 32–39.
- [9] A. L. Desbiens, M. Pope, F. Berg, Z. E. Teoh, J. Lee, and M. Cutkosky, "Efficient jumpgliding: Theory and design considerations," *IEEE Int. Conf. Robot. Autom.*, pp. 4451–4458, 2013.
- [10] C. T. Farley, J. Glasheen, and T. A. McMahon, "Running springs: speed and animal size," *Jnl. Exp. Biol.*, vol. 185, pp. 71–86, 1993.
- [11] C. Gehring, S. Coros, M. Hutter, and R. Siegwart, "An optimization approach to controlling jump maneuvers for a quadrupedal robot," *Dyn. Walk.*, 2015.
- [12] D. W. Haldane, M. M. Plecnik, J. K. Yim, and R. S. Fearing, "Robotic vertical jumping agility via series-elastic power modulation," *Sci. Robot.*, vol. 1, no. 1, 2016.
- [13] D. W. Haldane, M. Plecnik, J. K. Yim, and R. S. Fearing, "A power modulating leg mechanism for monopodal hopping," *IEEE Int. Conf. Intell. Robot. Syst.*, pp. 4757–4764, 2016.
- [14] G. C. Haynes, J. Pusey, R. Knopf, A. M. Johnson, and D. E. Koditschek, "Laboratory on legs: an architecture for adjustable morphology with legged robots," University of Pennsylvania, Philadelphia, PA, Tech. Rep., 2012.
- [15] P. E. Hudson, S. a. Corr, and A. M. Wilson, "High speed galloping in the cheetah (*Acinonyx jubatus*) and the racing greyhound (*Canis familiaris*): spatio-temporal and kinetic characteristics," *J. Exp. Biol.*, vol. 215, no. 14, pp. 2425–34, 2012.
- [16] F. Iida, R. Dravid, and C. Paul, "Design and control of a pendulum driven hopping robot," in *IEEE Int. Conf. Intell. Robot. Syst.*, 2002, pp. 2141–2146.
- [17] A. M. Johnson and D. E. Koditschek, "Toward a vocabulary of legged leaping," *IEEE Int. Conf. Robot. Autom.*, pp. 2568–2575, 2013.
- [18] G.-P. Jung, C. S. Casarez, S.-P. Jung, R. S. Fearing, and K.-J. Cho, "An integrated jumping-crawling robot using height-adjustable jumping module," *IEEE Int. Conf. Robot. Autom.*, pp. 4680–4685, 2016.
- [19] G. Kenneally, A. De, and D. E. Koditschek, "Design principles for a family of direct-drive legged robots," *IEEE Robot. Autom. Lett.*, vol. 1, no. 2, pp. 900–907, 2016.
- [20] M. Kovac, M. Fuchs, A. Guignard, J.-C. Zufferey, and D. Floreano, "A miniature 7g jumping robot," in *IEEE Int. Conf. Robot. Autom.*, 2008, pp. 373–378.
- [21] M. Kovač, Wassim-Hraiz, O. Fauria, J. C. Zufferey, and D. Floreano, "The EPFL jumpglider: A hybrid jumping and gliding robot with rigid or folding wings," *IEEE Int. Conf. Robot. Biomimetics*, pp. 1503–1508, 2011.
- [22] F. Li, W. Liu, X. Fu, G. Bonsignori, U. Scarfogliero, C. Stefanini, and P. Dario, "Jumping like an insect: Design and dynamic optimization of a jumping mini robot based on bio-mimetic inspiration," *Mechatronics*, vol. 22, no. 2, pp. 167–176, 2012.
- [23] M. Noh, S.-W. Kim, S. An, J.-S. Koh, and K.-J. Cho, "Flea-Inspired Catapult Mechanism for Miniature Jumping Robots," *IEEE Trans. Robot.*, vol. 28, no. 5, pp. 1007–1018, 2012.
- [24] H. W. Park, S. Park, and S. Kim, "Variable-speed quadrupedal bounding using impulse planning: Untethered high-speed 3D Running of MIT Cheetah 2," in *IEEE Int. Conf. Robot. Autom.*, vol. 2015-June, no. June, 2015, pp. 5163–5170.
- [25] M. M. Plecnik, D. W. Haldane, J. K. Yim, and R. S. Fearing, "Design exploration and kinematic tuning of a power modulating jumping monopod," *J. Mech. Robot.*, vol. 9, pp. 1–13, 2016.
- [26] M. H. Raibert, H. B. Brown, and M. Chepponis, "Experiments in balance with a 3D one-legged hopping machine," *Int. J. Rob. Res.*, vol. 3, no. 2, pp. 75–92, 1984.
- [27] A. Sayyad, B. Seth, and P. Seshu, "Single-legged hopping robotics research - A review," *Robotica*, vol. 25, no. 05, pp. 587–613, 2007.
- [28] S. A. Stoeter, P. E. Rybski, M. Gini, and N. Papanikopoulos, "Autonomous stair-hopping with scout robots," *IEEE Int. Conf. Intell. Robot. Syst.*, vol. 1, pp. 721–726, 2002.
- [29] T. Tsuda, H. Mochiyama, and H. Fujimoto, "Quick stair-climbing using snap-through buckling of closed elastica," *Int. Symp. Micro-NanoMechatronics Hum. Sci.*, pp. 368–373, 2012.
- [30] T. Wei, G. Nelson, and R. Quinn, "Design of a 5-cm monopod hopping robot," *IEEE Int. Conf. Robot. Autom.*, pp. 2828–2833, 2000.
- [31] B. Weiss, "Hop Hopbots!" *Sci. News*, vol. 159, 2001.
- [32] M. A. Woodward and M. Sitti, "MultiMo-Bat: A biologically inspired integrated jumping-gliding robot," *Int. J. Rob. Res.*, vol. 33, pp. 1511–1529, 2014.
- [33] V. Zaitsev, O. Gvirsman, U. Ben Hanan, A. Weiss, A. Ayali, and G. Kosa, "Locust-inspired miniature jumping robot," in *IEEE Int. Conf. Intell. Robot. Syst.*, 2015, pp. 553–558.
- [34] G. Zeglin and H. B. Brown, "First Hops of the 3D Bow Leg Hopper," *5th Int. Conf. Climbing Walk. Robot.*, pp. 357–364, 2002.
- [35] J. Zhao, N. Xi, B. Gao, M. W. Mutka, and L. Xiao, "Development of a controllable and continuous jumping robot," *IEEE Int. Conf. Robot. Autom.*, pp. 4614–4619, 2011.